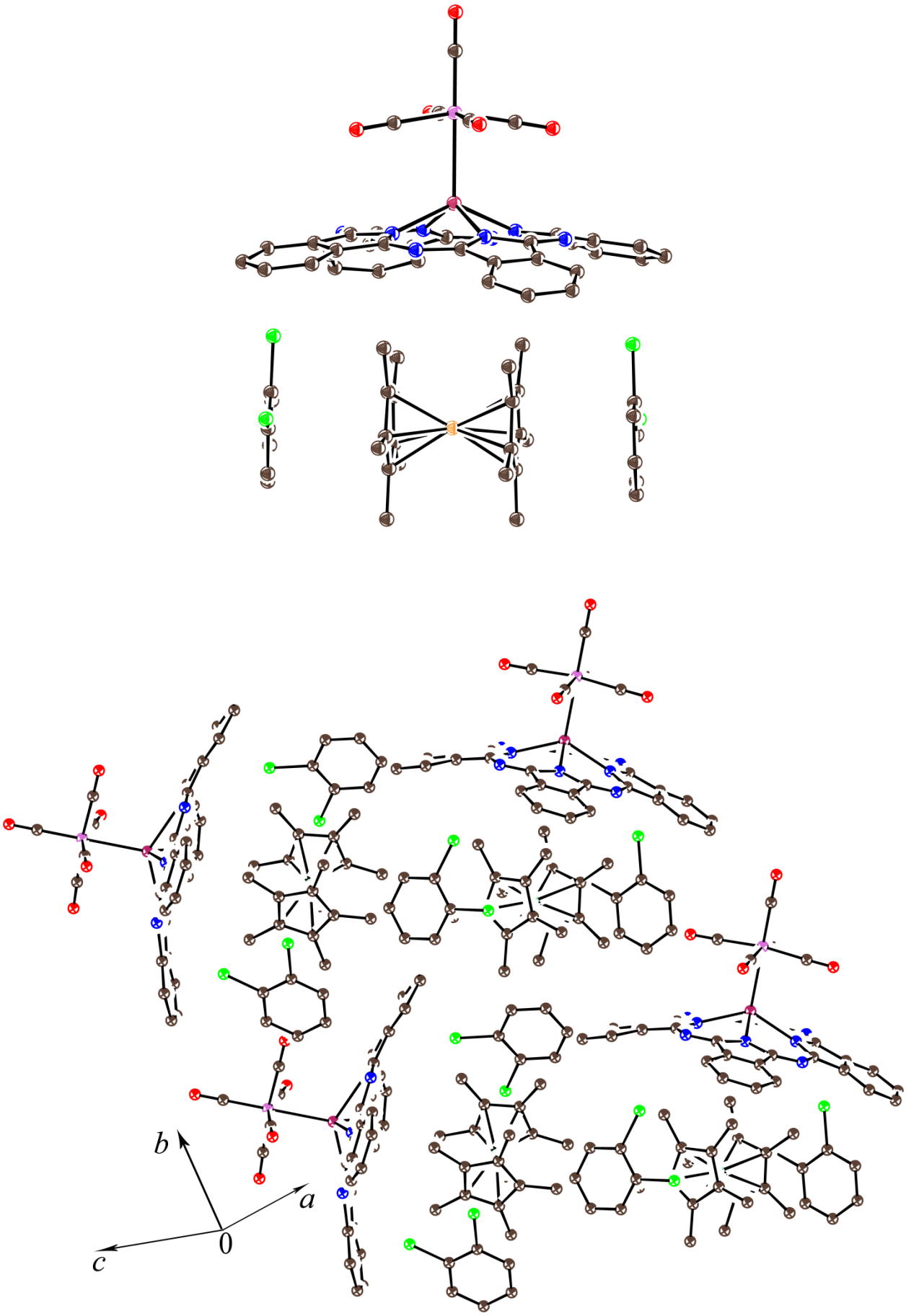

Figure S1. Crystal structure of $(Cp^*_2Cr^+)\{[Mn(CO)_5]^-[In^{III}(Pc^{\bullet 3-})]\}\cdot 2C_6H_4Cl_2$ (**2**)

Table S1. IR spectra of starting compounds and complexes **1** and **2**

Components	InClPc	$[Co(CO)_4]_2$	$\{[Co(CO)_4]^-$ $[In^{III}(Pc^{2-})]\}$ (**1**)	$[Mn(CO)_5]_2$	Cp^*_2Cr	$(Cp^*_2Cr^+)$ $\{[Mn(CO)_5]^-$ $[In^{III}(Pc^{\bullet 3-})]\}\cdot$ $2C_6H_4Cl_2$ (**2**)
InClPc	437w 497w 570m 634w 663w 724s 749m 771m 780m 802w 836w 885m 959w 1003w 1059s 1083s 1118s 1160m 1284s 1332s 1408m 1473s 1608w 1645w 3047w		430w* - 570w - - 724s 749m 773m - - - 887m - - 1063m 1081s 1117s 1162w 1285w 1332s 1409w 1476m 1597w - -		-	438w 489w 569w* - 667m* 714w 746m* 762w - - 827w 886w - - 1061w* 1089m 1112s* 1165m 1284w 1331w - 1459s* - - -
Transition metal fragment	-	416s 477s 503s 524s 543s CO 1843s 1896s 2003s	430w* - - 519w 551m CO 1975s 2010s 2080s	449m 467m 547w 577w 591w 639s 665m CO 1997s 2020s -	-	- - - 569w* - - 667m* CO 1974s - 2077s
Cp^*_2Cr	-	-	-	-	587w 800w 1019m 1067w 1262w 1375m 1417w 1446w 2851w 2955w	- - - 1061w* - - 1421m - - -
Solvent	-	-	-	-	-	$C_6H_4Cl_2$ 667m* 747m* 1036w 1112s* 1459s*

* - bands are coincided; w – weak, m –middle and s – strong intensity

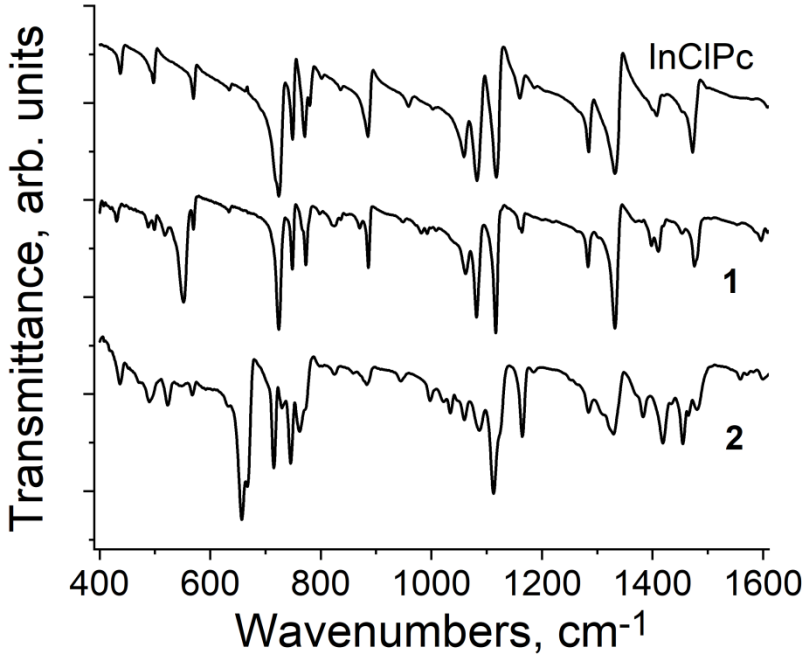

Figure S2. IR spectra of starting neutral InClPc and salts **1** and **2** in KBr pellets prepared in anaerobic condition.

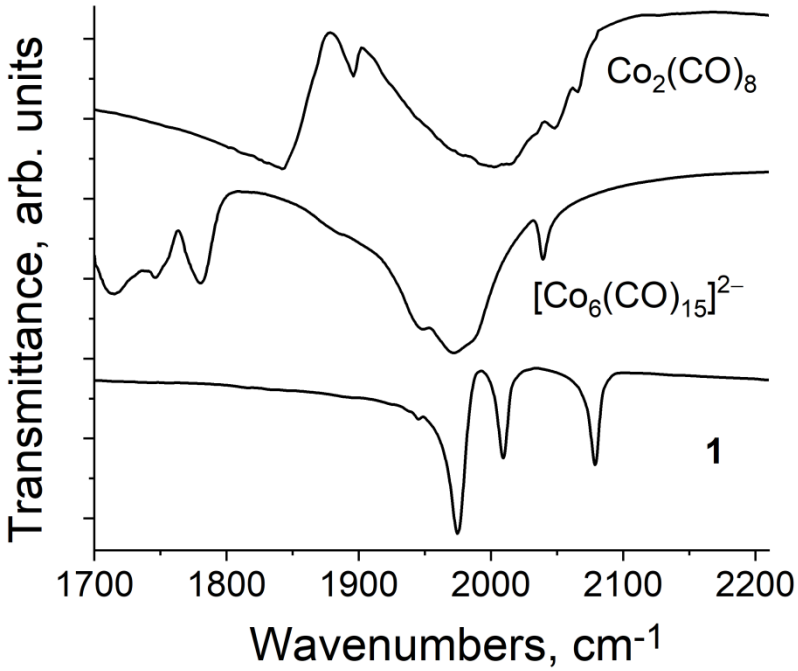

Figure S3. IR spectra of starting transition metal $[Co(CO)_4]_2$, anionic metal carbonyl cluster in $\{DB\text{-}18\text{-}crown\text{-}6(Na^+)\}_2[Co_6(CO)_{15}]^{2-}\cdot 2C_6H_4Cl_2$ [1] and complex **1** in 1700 – 2200 cm^{-1} range in KBr pellets prepared in anaerobic conditions

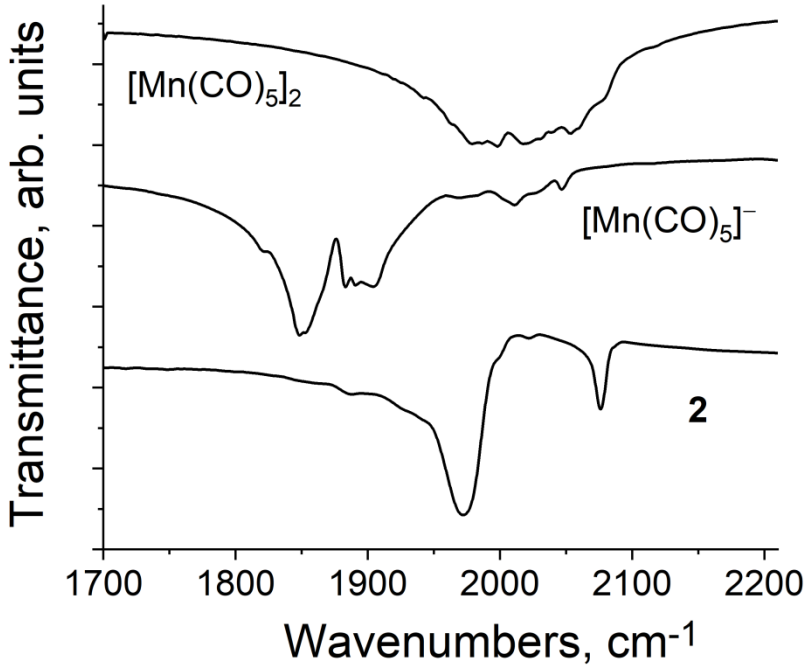

Figure S4. IR spectra of starting transition metal $[Mn(CO)_5]_2$ carbonyl, anionic metal carbonyl in $(Cp^*_2Cr^+)[Mn(CO)_5]^-$ [1] and complex **2** in 1700 – 2200 cm^{-1} range in KBr pellets prepared in anaerobic conditions.

Magnetic data for **2**.

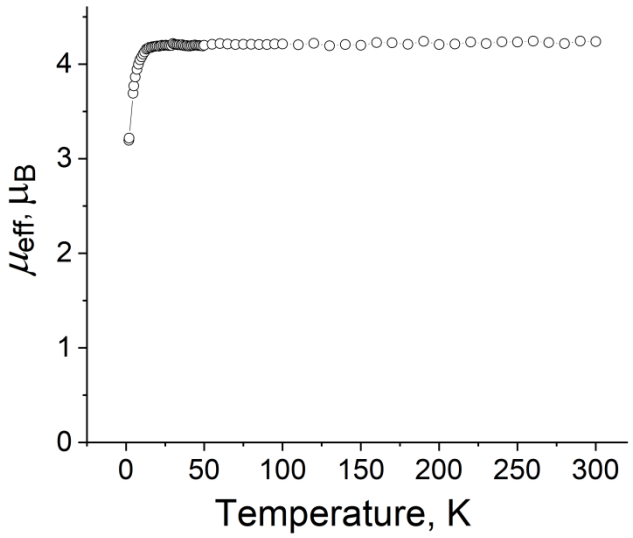

Figure S5. Temperature dependence of an effective magnetic moment of polycrystalline **2** measured in anaerobic conditions

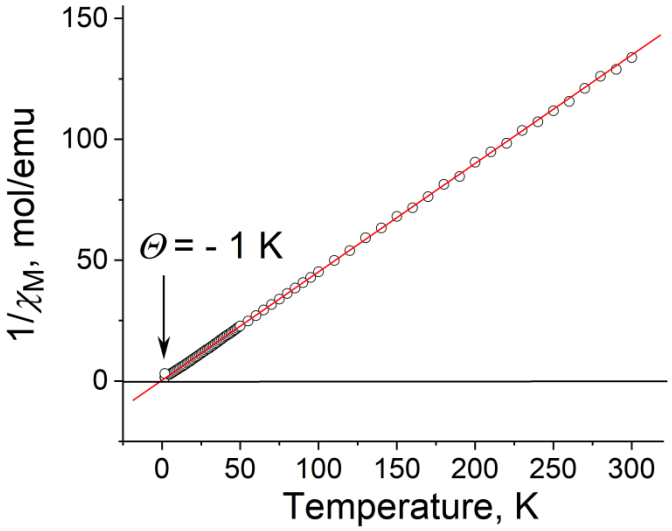

Figure S6. Temperature dependence of the reciprocal molar magnetic susceptibility of polycrystalline **2** measured in anaerobic conditions. Approximation of data by the Curie-Weiss law is shown by red line.

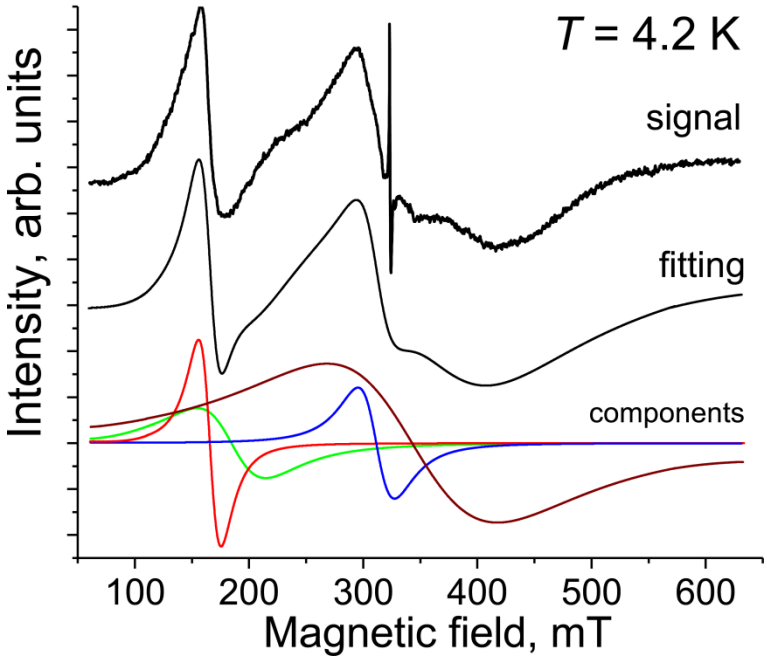

Figure S7. EPR spectrum of the polycrystalline sample of **2** at 4.2 K measured in an anaerobic conditions. Frequency 9.05870 GHz, microwave power 1 mW, amplitude 320, modulation width 0.2 mT.

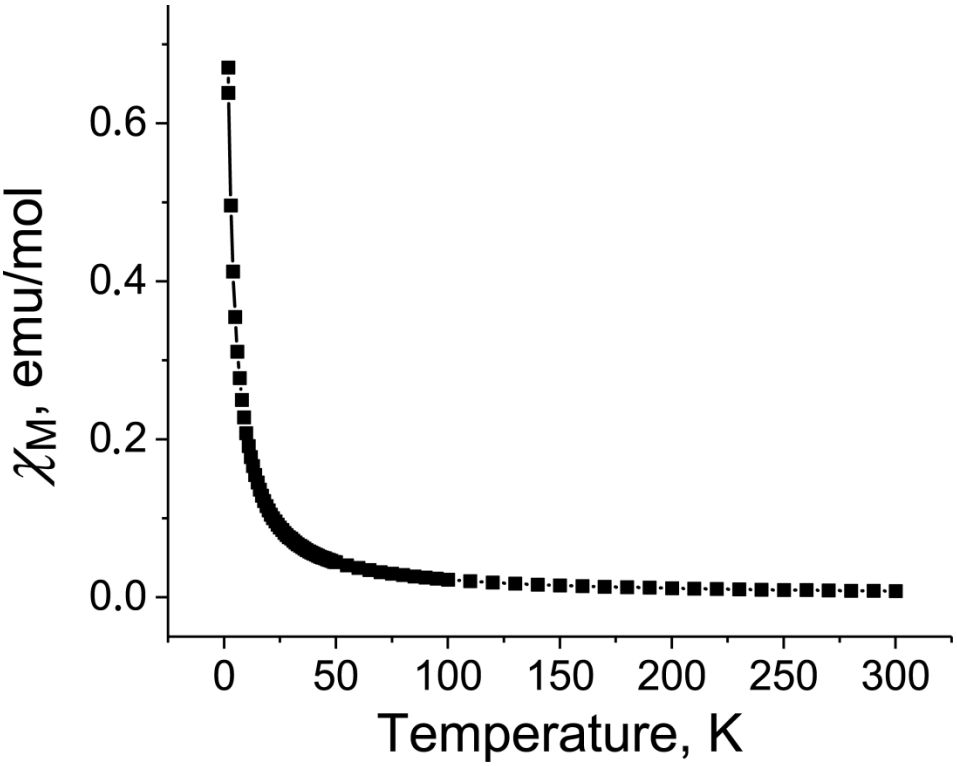

Figure S8. Temperature dependence of molar magnetic susceptibility of polycrystalline **2** measured in anaerobic conditions.

References

1. Konarev DV, Kuzmin AV, Galkin RS, Khasanov SS, Kurbanov RF, Otsuka A, et al. Salts of Anionic Metal Carbonyl Clusters with Cryptand[2.2.2](Na $^{+}$), DB-18-crown-6(Na $^{+}$), and Paramagnetic Cp* $_{2}$ Cr $^{+}$ Cations Obtained by Reduction: Salts of Anionic Metal Carbonyl Clusters with Cryptand[2.2.2](Na $^{+}$), DB-18-crown-6(Na $^{+}$), and Paramagnetic Cp* $_{2}$ Cr $^{+}$ Cations Obtained by Reduction. Z Anorg Allg Chem 2019; 645:472–83. https://doi.org/10.1002/zaac.201800463